Biosensors and Bioelectronics 28 (2011) 407–413

Contents lists available at ScienceDirect

Biosensors and Bioelectronics

journal homepage: www.elsevier.com/locate/bios

Characterization and application of a surface modification designed for QCM-D studies of biotinylated biomolecules

Erik Nilebäck[a,b,*], Laurent Feuz[a], Hans Uddenberg[b], Ramūnas Valiokas[c], Sofia Svedhem[a]

[a] Division of Biological Physics, Department of Applied Physics, Chalmers University of Technology, SE-412 96 Göteborg, Sweden
[b] Q-Sense, Hängpilsgatan 7, SE-426 77 Västra Frölunda, Sweden
[c] Department of Nanoengineering, Center for Physical Sciences and Technology, Savanoriu 231, LT-02300 Vilnius, Lithuania

ARTICLE INFO

Article history:
Received 1 June 2011
Received in revised form 11 July 2011
Accepted 21 July 2011
Available online 30 July 2011

Keywords:
QCM-D
Self-assembled monolayer
Biotin
Streptavidin
Biosensor
Biomolecular interactions

ABSTRACT

The rapid development of surface sensitive biosensor technologies, especially towards nanoscale devices, requires increasing control of surface chemistry to provide reliable and reproducible results, but also to take full advantage of the sensing opportunities. Here, we present a surface modification strategy to allow biotinylated biomolecules to be immobilized to gold coated sensor crystals for quartz crystal microbalance with dissipation monitoring (QCM-D) sensing. The unique feature of QCM-D is its sensitivity to nanomechanical (viscoelastic) properties at the sensing interface. The surface modification was based on mixed monolayers of oligo(ethylene glycol) (OEG) disulfides, with terminal –OH or biotin groups, on gold. Mixtures containing 1% of the biotin disulfide were concluded to be the most appropriate based on the performance when streptavidin was immobilized to biotinylated sensors and the subsequent biotinylated bovine serum albumin (BSA) interaction was studied. The OEG background kept the unspecific protein binding to a minimum, even when subjected to serum solutions with a high protein concentration. Based on characterization by contact angle goniometry, ellipsometry, and infrared spectroscopy, the monolayers were shown to be well-ordered, with the OEG chains predominantly adopting a helical conformation but also partly an amorphous structure. Storage stability was concluded to depend mainly on light exposure while almost all streptavidin binding activity was retained when storing the sensors cold and dark for 8 weeks. The surface modification was also tested for repeated antibody–antigen interactions between BSA and anti-BSA (immobilized to biotinylated protein A) in QCM-D measurements lasting for >10 h with intermediate basic regeneration. This proved an excellent stability of the coating and good reproducibility was obtained for 5 interaction cycles. With this kind of generic surface modification QCM-D can be used in a variety of biosensing applications to provide not only mass but also relevant information of the structural properties of adlayers.

1. Introduction

Biosensing platforms based on surface sensitive analytical techniques is an emerging field of research, where the development of more and more advanced surface modifications allows the study of biomolecular interactions in increasingly complex local environments (Collings and Caruso, 1997; Jonkheijm et al., 2008; Luppa et al., 2001). Common biosensor detection principles are based on changes in optical or viscoelastic properties at the sensor interface caused by binding of biomolecules (Cooper, 2003). Since biosensing is an indirect method where changes in global properties are measured as opposed to direct molecular information it is of vital importance to properly control the composition of the sensor interface to specifically detect the interaction of interest. Optical biosensing has proven very successful in the field of protein–protein and drug–protein interaction studies and primarily techniques based on surface plasmon resonance (SPR) have been used extensively for drug screening for many years (Hoa et al., 2007; Vuignier et al., 2010; Zhu and Cuozzo, 2009). The acoustic quartz crystal microbalance with dissipation monitoring (QCM-D) technique is still underexplored in this context, perhaps mostly due to the moderate mass sensitivity of 1 ng/cm^2 often used as an argument for why QCM-D cannot be used to detect binding of small drug molecules. However, we recently published a study where small drug molecules (<160 Da) interacted with the protein drug target plasminogen (~85 kDa) to induce a large conformational change of the protein which was detected as energy dissipation changes with QCM-D but not as mass changes in SPR (Nileback et al., 2010). This is an example where the change in nanomechanical properties was more prominent than the actual amount

* Corresponding author at: Division of Biological Physics, Department of Applied Physics, Chalmers University of Technology, Fysikgrand 3, SE-412 96 Göteborg, Sweden.
E-mail address: nileback@chalmers.se (E. Nilebäck).

0956-5663/$ – see front matter © 2011 Elsevier B.V. All rights reserved.
doi:10.1016/j.bios.2011.07.060

of bound drug molecules. Similarly, covalent end-on immobilization of small peptides to supported lipid bilayers has proven to be readily detected by QCM-D although hardly possible to detect by optical techniques (Edvardsson et al., 2009). We argue that a major reason for QCM-D not being used more often in e.g. drug discovery is the lack of easily accessible substrates for protein immobilization.

One common strategy to control biomolecule immobilization to sensor surfaces is to take advantage of the strong interaction between streptavidin, secreted by the bacteria *Streptomyces avidinii*, and biotin which has one of the highest non-covalent affinities known with a $K_d \approx 10^{-14}$–10^{-16} M (Hendrickson et al., 1989; Laitinen et al., 2006; Wilchek and Bayer, 1988, 1999). Streptavidin is a 60 kDa, tetrameric protein, with a slightly acidic isoelectric point (pI) of ~5.5 and four binding sites for the small vitamin biotin (244 Da) (Vermette et al., 2003; Wilchek and Bayer, 1988, 1999). From crystal structures, the geometry of streptavidin is commonly approximated by a cube with the side length of 4.75 Å (Hendrickson et al., 1989). Additional reasons to the popularity of streptavidin in biotechnology are that the protein is highly resistant to changes in pH, temperature, and exposure to denaturing agents, allowing a variety of experimental conditions to be used (Laitinen et al., 2006). Streptavidin belongs to a common class of biotin-binding proteins, available both from natural sources (avidin (pI ~10) is extracted from egg white) and as bioengineered products. Neutravidin is a deglycosylated variant of avidin which is neutral at neutral pH (pI ~6.5) (Vermette et al., 2003; Wolny et al., 2010b), and other avidin or streptavidin variants showing altered affinity properties have been developed (Laitinen et al., 2006). Biotin–streptavidin systems have been used in a variety of application fields such as screening (Huang et al., 2001; Prieto-Simon et al., 2008; Welch et al., 1996), DNA hybridization (Aung et al., 2008; Hook et al., 2001; Larsson et al., 2003), patterning (Zhang et al., 2010), polymers (Huang et al., 2002; Richter et al., 2007; Wolny et al., 2010a), and protein interactions (Lee et al., 2005). This wide range of applications makes biotinylated sensor surfaces attractive for almost all surface based sensing techniques and the aim of this study was to develop and characterize biotinylated surfaces for the QCM-D technique.

To properly biotinylate sensor surfaces, it is important to reduce contributions from non-specific interactions at the sensor surface. For SPR-based sensing, biotin surface modifications typically involve the modification of a hydrogel on the sensor surface to optimally take advantage of the sensing volume. For the QCM-D technique, which is sensitive to viscoelastic changes near the sensor surface, results will be more difficult to interpret when involving polymeric layers due to swelling or de-swelling of the hydrogel, and therefore a requirement for the present design was to have the biotin localized close to the sensor surface. This feature is also important for localized SPR sensing (LSPR), where the sensing depth is much shorter (~15 nm) compared to conventional SPR setups (~200 nm).

In this study, we have chosen to work with mixtures of short oligo(ethylene glycol) (OEG) disulfides with 7–9 ethylene glycol units containing a certain fraction with biotinylated end groups. The short OEG chains were chosen before the longer poly(ethylene glycol) (PEG) chains to minimize viscoelastic interference with the QCM-D results (Nileback et al., 2010). The present study provides thorough characterization of the sensor modification by several analytical techniques (contact angle goniometry, infrared spectroscopy, and ellipsometry), and also a new application example where repeated antigen–antibody interactions between bovine serum albumin (BSA) and anti-BSA were studied reproducibly in an automated QCM-D setup.

2. Experimental

2.1. Materials

AT-cut 5 MHz quartz crystals (QCM-D sensors) sputter-coated with a 100 nm thick Au layer onto a 50 nm chromium adhesive layer were obtained from Q-Sense AB, Sweden. Symmetric OEG disulfides with terminal hydroxyl (dS-OEG, structure: $-(S-CH_2-(CH_2-O-CH_2)_7-CH_2-OH)_2$, MW: 771.0 Da) or biotin groups (dS-OEG-biotin, structure: $-(S-C_2H_4-CO-NH-(CH_2-O-CH_2)_9-NH-CO-C_4H_8-\text{Biotin})_2$ MW: 1539.9 Da) were purchased from Polypure, Norway. Phosphate buffered saline (PBS) contained 137 mM NaCl, 2.7 mM KCl and 10 mM phosphate, pH 7.4 (Sigma) and Hepes buffered saline (HBS) contained 150 mM NaCl, 10 mM Hepes, pH 7.4 (GE Healthcare). Fetal bovine serum (FBS) was purchased from PAA Laboratories, Austria. Streptavidin, biotinylated and non-biotinylated bovine serum albumin (biotin-BSA, BSA), biotinylated protein A (biotin-protein A), anti bovine serum albumin IgG polyclonal antibody (anti-BSA) and additional chemicals were purchased from Sigma–Aldrich. Ethanol was of spectroscopic grade. Protein solutions were prepared by dilution in buffer and stored at <−20 °C prior to use. Water was purified and deionized to a resistivity of >18.2 MΩ cm with a Milli-Q system (MilliPore, France).

2.2. Preparation of sensor surface modification

Gold-coated QCM-D sensors were cleaned in a 5:1:1 solution of water, 25% ammonia and 30% hydrogen peroxide for 10 min at 80 °C prior to disulfide incubation. After rinsing of the surfaces repeatedly with water they were dried under a flow of nitrogen and placed in an ethanolic 0.5 mM disulfide solution of dS-OEG with varying mole fraction (ranging from 0.01% to 10%) of dS-OEG-biotin for incubation >12 h to create mixed self-assembled monolayers of the disulfides on the gold coated sensors. After incubation, the sensors were rinsed in ethanol and ultra-sonicated for 3–5 min in ethanol to remove any non-covalently bound disulfides before measurement or storage.

For storage studies, biotinylated sensors were prepared as described above from an incubation solution with 1% biotin content and stored at room temperature sealed and non-sealed to light exposure and also dark at 2–8 °C. Duplicate samples were retrieved after 2, 4 and 8 weeks of storage and tested in QCM-D for streptavidin and biotin-BSA binding as described below.

2.3. Procedures for protein interaction studies by QCM-D

Non-specific protein binding was tested by exposing the modified sensors to non-diluted serum (FBS, total protein concentration of 30–45 mg/ml) for 30–60 min under static conditions in QCM-D, followed by rinsing with HBS. The amount of adsorbed serum proteins was measured relative to the HBS baseline obtained prior to the addition of serum. Similarly, biotinylated sensors were exposed to streptavidin (25 μg/ml in HBS) under flow (100–500 μl/min), until saturation was reached. After rinsing, the sensors were subjected to biotin-BSA (100 μg/ml in HBS).

Antigen–antibody interaction experiments were performed on three parallel biotinylated (1%) sensors under continuous flow (50–100 μl/min) in the Q-Sense E4 Auto instrument. The following sequence was employed for the immobilization of the antibody to the biotinylated sensor via protein A (all protein solutions diluted in PBS); (i) stabilization of the baseline in PBS (20 min), (ii) streptavidin (25 μg/ml, 10 min), (iii) biotin-protein-A (25 μg/ml, 10 min), (iv) anti-BSA (10 μg/ml, 20 min), and (v) BSA (50 μg/ml, 20 min).

Experiments were run in duplicates with a single additional negative control where PBS was flown instead of

biotin-protein-A, anti-BSA and BSA to test the stability of the biotinylated sensor surface. The antibody–antigen complex was removed using 10 mM NaOH in water, after which more antibody was again immobilized to the surface for another experiment. Rinsing was performed with PBS for at least 10 min at 100 μl/min between each immobilization or regeneration step.

All QCM-D measurements were performed with an E4 Q-Sense instrument with four parallel flow modules that allowed for up to four simultaneous real-time measurements under flow. In some experiments, an automated setup (E4 Auto, Q-Sense) of the QCM-D instrument allowing automatic and pre-programmed sample retrieval was used. The flow was controlled by an Ismatec IPC-N 4 peristaltic pump that produced stable flows in the range 50–500 μl/min. All measurements were performed at a controlled temperature of 22 °C, using degassed solutions. Frequency shifts were normalized by division with the corresponding overtone number. Data was collected at the fundamental frequency and at several overtones. The variation between the overtone signals was small and therefore only the 7th overtone will be shown in the QCM-D results.

2.4. Contact angle goniometry

Static contact angle measurements were performed with a Krüss DSA10 goniometer using a 5 μl sessile drop of water, and the data was analyzed with the software DSA1 Drop shape analysis.

2.5. Ellipsometry

Variable angle spectroscopic ellipsometry was performed with a rotating compensator ellipsometer of the type M2000-F™ (J.A. Woollam Co., Inc., Lincoln, Nebraska, USA) for wavelengths ranging from 380 to 1000 nm and for angles of incidence of 65°, 70° and 75°. To calculate the film thickness, d, of the surface modifications, a Cauchy model with $A_0 = 1.45$, $B_0 = 0.01$ and $C_0 = 0$ was used as an estimate for the refractive index of the thin organic film.

2.6. Infrared spectroscopy

Reflection–absorption (RA) spectra were recorded on a Bruker Tensor 27 infrared spectrometer, equipped with a Hyperion 3000 FT-IR microscope with a stage to allow measurements on gold coated QCM-D crystals. A grazing angle of 85° and a liquid nitrogen cooled-MCT detector were used. The measurement chamber was continuously purged with nitrogen gas during the measurements. The acquisition time was approximately 15 min. The RA spectra were recorded at 8 cm^{-1} resolution and a three-term Blackmann–Harris apodization function was applied to the interferograms before Fourier transformation. A spectrum of a deuterated hexadecane thiol ($HS(CD_2)_{15}CD_3$) monolayer on a gold coated QCM-D crystal was recorded and used as a reference.

3. Results and discussion

3.1. Optimization of surface chemistry with respect to biotin fraction

The first step in the development of the biotin sensor coating was to find the fraction of the biotin disulfide that was required for optimal performance. Two parameters were evaluated; (i) the amount of streptavidin which bound to the biotinylated surfaces, and (ii) the amount of biotin-BSA which was subsequently immobilized to the streptavidin-modified surface. Streptavidin and biotin-BSA were chosen as a test system for both the surface chemistry optimization and storage studies since it is a stable, cheap, and well-documented system for different applications (Aung et al., 2008; Gobi et al., 2007; Rindzevicius et al., 2005; Wolny et al., 2010b). The results for a series of experiments with fractions of biotin disulfide ranging from 0.01% to 10% in the incubation solution are shown in Fig. 1.

For optimal sensor performance it is crucial to achieve immobilization of a full monolayer of streptavidin to maximize the number of exposed biotin-binding sites for additional biotinylated molecules (Edvardsson et al., 2009; Huang et al., 2002; Richter et al., 2007). The formation of a complete monolayer can be seen in Fig. 1a for biotin concentrations ≥ 0.7% where the streptavidin immobilization has saturated at frequency shifts of $-22\,Hz \pm 3\,Hz$ and with low dissipation shifts, $0.1 \times 10^{-6} \pm 0.1 \times 10^{-6}$. These values are in the range of earlier reported values for streptavidin monolayer formation measured by QCM-D on biotinylated alkane thiols (Azzaroni et al., 2007; Seifert et al., 2010), poly-L-lysine-PEG layers (Huang et al., 2002) and supported lipid bilayers (Bingen et al., 2008; Edvardsson et al., 2009; Hook et al., 2001; Larsson et al., 2003). For surface modifications using lower fractions of the biotin disulfide (0.01–0.1%), sub-monolayer coverages of immobilized streptavidin were obtained, in turn resulting in substantially less binding of biotin-BSA. For large fractions of biotin (10%), a monolayer of streptavidin was immobilized, but less of the subsequently added biotin-BSA was bound compared to the optimal biotin fraction on the sensor surface at 1%. This is likely due to either steric blocking of biotin binding sites between too close-packed streptavidin molecules or to the large availability of biotin which enhances the risk that all binding sites on streptavidin are occupied by surface exposed biotin prior to the exposure to biotin-BSA. The latter mechanism was previously reported for surface modifications with longer PEG chains (Huang et al., 2002) and is less likely to be the dominant effect in the present protocol that uses very short OEG chains.

Based on these results we chose to continue to use the disulfide solution with 1% biotin content. This allowed a monolayer of streptavidin to be formed without approaching the steep reduction in protein bound to the surface seen from 0.7% and below in Fig. 1a and from 0.4% and below in Fig. 1b. The typical and very reproducible profiles of the frequency and dissipation shifts for streptavidin and subsequent biotin-BSA adsorption on monolayers with 1% biotin content are shown in Fig. 2.

As can be seen in Fig. 2 both frequency and dissipation signals were very stable. Both streptavidin and biotin-BSA were bound with fast kinetics which is to expect due to their high affinity and the concentration being high at 25 μg/ml. It was possible to perform the adsorption at flow rates ranging from 50 to 500 μl/min with the same end result. The significant peak seen in the dissipation for the streptavidin adsorption at ~12 min in Fig. 2b has been discussed in detail elsewhere for supported lipid bilayers, and was first suggested to be due to rearrangements in the streptavidin layer on the laterally mobile membrane leading to the formation of a crystalline, rigid layer resulting in a lower dissipation (Hook et al., 2001; Reviakine and Brisson, 2001). However, for the present biotinylated sensors this dissipation decrease is most likely due to the bound streptavidin having some space to move at low coverages, most likely in a rocking motion, until higher coverage forces them to arrange in a more rigid 2D layer because of increased hydrodynamic interactions between neighboring proteins and thus decreased mobility in the linker, as was also suggested in a more recent study on supported lipid membranes (Johannsmann et al., 2009). This phenomenon was rather unexpected in the present study since the disulfide monolayer does not possess the lateral mobility of supported lipid bilayers. The significant peak in dissipation, however, suggests that the flexibility of the OEG chains is sufficient to allow for the streptavidin molecules to inter-molecularly rearrange at the sensor surface.

Non-specific protein adsorption to the 1% biotinylated sensors was tested in two ways; (i) fetal bovine serum (FBS) adsorption to

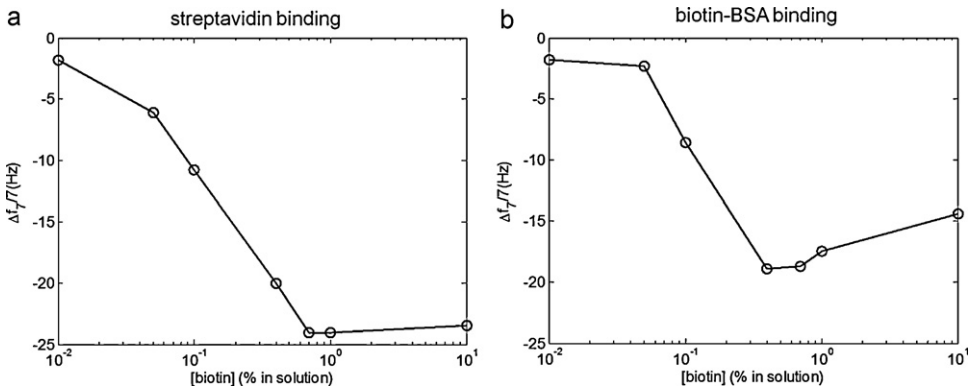

Fig. 1. Amount of (a) bound streptavidin and (b) subsequently bound biotin-BSA as determined by the corresponding QCM-D frequency shifts as a function of biotin fraction in the incubation solution during sensor surface modification. The lines were drawn as a guide for the eye. The standard deviation in these experiments was typically <1 Hz, based on many replicates of the streptavidin and biotin-BSA immobilizations on 1% biotinylated sensors.

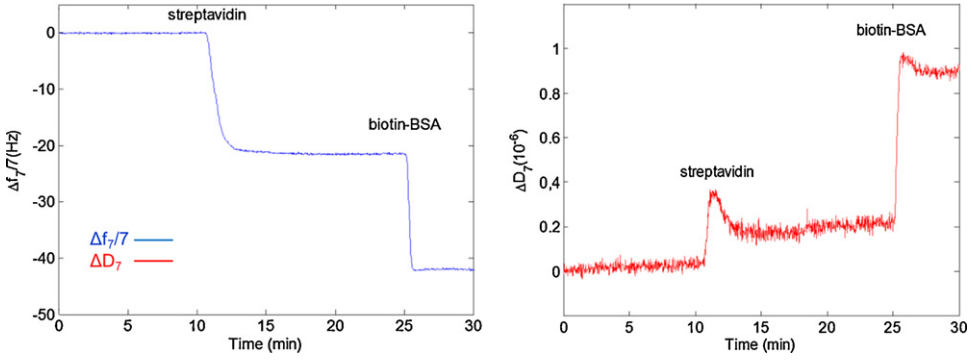

Fig. 2. QCM-D (a) frequency and (b) dissipation shifts for the sequential binding of streptavidin and biotin-BSA on 1% biotinylated sensor surfaces. The shifts for streptavidin ($\Delta f = -22 \pm 3$ Hz; $\Delta D = 0.1 \times 10^{-6} \pm 0.1 \times 10^{-6}$) and biotin-BSA ($\Delta f = -18 \pm 2$ Hz; $\Delta D = 0.7 \times 10^{-6} \pm 0.1 \times 10^{-6}$) were reproducible for >5 replicates.

freshly prepared sensors, and (ii) non-biotinylated BSA adsorption to streptavidin coated sensors before adsorption of biotin-BSA. The freshly prepared biotinylated sensors showed negligible adsorption (0.24 ± 1 Hz compared to -51 ± 24 Hz for clean gold) from the FBS (~30 mg/ml of protein) which is a strong indicator that the 7–9 EG units long OEG chains are sufficiently long and well-ordered to give the protein repellant properties typical for thiol-OEG derivatives (Palegrosdemange et al., 1991; Prime and Whitesides, 1993). When subjecting the streptavidin layer to non-biotinylated BSA, very small shifts of less than −1 Hz could be seen that were reversible upon rinsing proving that the streptavidin–biotin-BSA interactions measured were the results of specific interactions.

3.2. Storage stability of 1% biotinylated sensors

When developing and designing biosensor surfaces one important aspect is the robustness and stability of the surface modification over time. We therefore conducted a storage stability study of the binding activity over 8 weeks with intermediate tests at 0, 2 and 4 weeks with the results shown in Fig. 3. All sensors were stored in air and sealed in polystyrene boxes to exclude contaminations from the ambient environment.

In Fig. 3, the desired amounts of streptavidin (Fig. 3a) and biotin-BSA (Fig. 3b) binding have been indicated by the dashed line, which coincides with the amount bound at $t = 0$ weeks. Fig. 3 shows that the sensors stored cold and dark have the best storage stability with almost completely retained activity after 8 weeks of storage. The sensors stored dark at room temperature have partially lost their function after 8 weeks but still bind both streptavidin and biotin-BSA. Large variations were seen in the frequency shifts for the sensors stored in light at room temperature with a very low adsorption at 2 weeks of −5 Hz for the streptavidin and close to 0 Hz for the biotin-BSA. At 4–8 weeks large frequency shifts can be seen for the streptavidin binding to these sensors while the biotin-BSA amount is low (−3 and −7 Hz, respectively). One way of explaining this increase in streptavidin binding is by looking at the biotin-BSA/streptavidin ratio that is 0.28 for the light/RT stored sensors compared to 0.82 for all of the dark stored sensors. This reveals that most of the streptavidin bound to the light stored sensors is inactive which was also typically the case, in our experiments, when adsorbing streptavidin to an unmodified gold surface. This indicates that the surface modifications on the light stored sensors were degraded to a large extent. Light induced photo-oxidation of thiols have been reported earlier (Brewer et al., 2005), and such processes are the most likely explanation for the results in our storage tests where the most important parameter when storing the biotin modified sensors was to keep the sensors away from light.

3.3. Structural characterization of 1% biotinylated sensors

The OEG-disulfide biotinylated monolayers formed on the sensor surfaces were further characterized by water contact angle goniometry, ellipsometry, and infrared reflection–absorption spectroscopy (IRRAS).

Table 1
Static water contact angle, Θ_c, and thickness measured by ellipsometry (in air), d (Å), for 1% biotinylated OEG monolayers.

Substrate	Θ_c (°)	d (Å)
OEG-biotin (1% biotin)	34 ± 1	15 ± 1

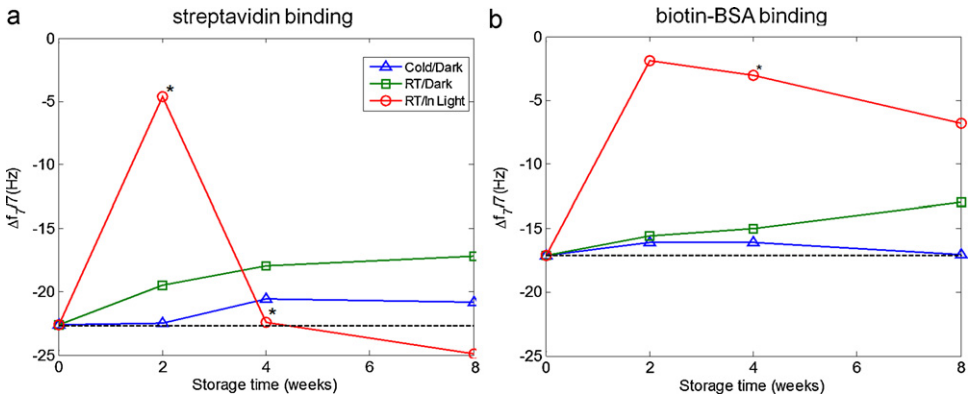

Fig. 3. QCM-D frequency shifts for (a) the immobilization of streptavidin and (b) the subsequent binding of biotin-BSA on 1% biotinylated sensors stored for 0, 2, 4 or 8 weeks cold and dark in the fridge (blue triangles), at room temperature (RT) and dark (green squares) or at RT exposed to ambient light (red circles). Lines were drawn to guide the eye. All samples were tested as duplicates and showed reproducible results with variations 1–12% except for the ones marked with * that had variations between ~40 and 100%. The dashed lines indicate the amount of streptavidin or biotin-BSA immobilized at 0 weeks. (For interpretation of the references to color in this figure legend, the reader is referred to the web version of the article.)

The water contact angle in Table 1 for the OEG-biotin modified sensors corresponded well to earlier reported values for OEG self-assembled monolayers, indicating that the monolayer is in a well-ordered state (Palegrosdemange et al., 1991; Prime and Whitesides, 1993). Dynamic measurements of the water contact angle were tested but differed with <5% in contact angle values from the static mode and therefore the static mode was chosen. The ellipsometric thickness was in the same range as earlier reported values for similar monolayers of thiolated OEG chains on gold (Vanderah et al., 2003, 2008) which indicate that most likely a single monolayer is present on the surface.

Furthermore, IRRAS was performed on the biotinylated sensors to investigate the conformation of the OEG chains. Helical and the more disordered amorphous conformations have been discussed to be important for protein repellant properties due to the way water molecules interact with the OEG chains in these conformations as compared to the non-protein repellant, close-packed all-trans conformation (Feldman et al., 1999; Harder et al., 1998; Vanderah et al., 2003, 2008). The strongly bound water layer acts as a barrier for protein adsorption since the water needs to be released before the OEG chains can interact with the protein. From literature, one expects peaks at 1114 cm^{-1} (C–O–C stretch), 1350 cm^{-1} (CH_2 wagging), and 2900 cm^{-1} (CH_2 asym. stretching) for helical OEG (Valiokas et al., 2009; Vanderah et al., 2003, 2008). In Fig. 4, these peaks are present but are shifted and broadened compared to literature values and this is likely due to a large portion of the OEG layer being in an amorphous phase. A likely explanation for this observation is the presence of biotin groups, where earlier studies had typically single molecule systems with a terminal CH_3 or OH and the more complex biotin group could then affect the IR adsorption in the OEG chains. It was not possible to detect the presence or concentration of biotin groups in the monolayer by the presence of an amide I peak at 1700 cm^{-1}, which is probably due to the low surface concentration of biotin and the inherent sensitivity limitations of infrared spectroscopy.

As has been discussed above and which can be seen in Fig. 3, the biotinylated sensors stored in light experienced a tremendous decrease in activity compared to those stored in light-sealed bags. To further investigate the molecular reasons behind this decrease in activity, parallel IRRAS measurements were performed on freshly prepared sensors with OEG-biotin (1% biotin) and compared to spectra from sensors stored for 10 days in light. By comparing the IRRAS spectra in Fig. 4 it can clearly be seen that the peak at 1114 cm^{-1} is substantially lower for the stored sample and the peaks at 2870 cm^{-1} and 1350 cm^{-1} are completely gone. This suggests that the layer has been severely degraded during storage in light which is also evident in the storage stability study of the binding efficiency seen in Fig. 3.

3.4. Performance in repeated antibody–antigen interaction studies

The biotinylated sensors were further studied with respect to stability in repeated protein interaction studies. A typical requirement for the present kind of surface chemistry designed for immobilization of any biotinylated molecule is to allow for extended experiments where immobilized proteins can be studied repeatedly and reproducibly over a long time. Therefore, long (>10 h) experiments of repeated antibody–antigen interactions were performed (Fig. 5) using a QCM-D setup with automated sample retrieval (E4 Auto) to test the stability of the sensors during conditions similar to a typical measurement in drug discovery applications. The test system was built upon repeated interactions between anti-BSA and BSA where the Fc-part of anti-BSA had been bound to biotinylated protein-A immobilized to a streptavidin monolayer.

The first steps in Fig. 5(I and II) look similar to the streptavidin and biotin-BSA binding shown in Fig. 2 except that the biotinylated protein-A induces a lower frequency shift than biotin-BSA. This is to be expected since the molecular weight of protein-A is ~50 kDa compared to ~66 kDa for BSA. The anti-BSA IgG induces large frequency and dissipation shifts which correlate well with the structure of an IgG protein at a molecular weight >150 kDa compared to the smaller BSA and protein-A. This has also been seen previously for unspecifically adsorbed BSA on platinum interacting with anti-BSA (Dolatshahi-Pirouz et al., 2008). The immobilized anti-BSA readily bound BSA with a high affinity, resisting rinsing with PBS, proving that the antibody was active on the surface. The BSA and anti-BSA could then be removed by 10 mM NaOH and all the steps III–V were repeated five times with very high reproducibility without any hands-on time using the automated system. These results prove that the biotinylated sensors can be used in a conventional screening setup allowing for regeneration solutions (here 10 mM NaOH) to be used several times without degrading the sensor coating. To our knowledge this is the first time that biotinylated sensors have been used for repeated antibody–antigen interactions studied by QCM-D, although this is a typical kind of experiment in SPR-based sensing. The presented biotin surface modification has also been used in a separate study where the conformational changes of biotinylated plasminogen upon

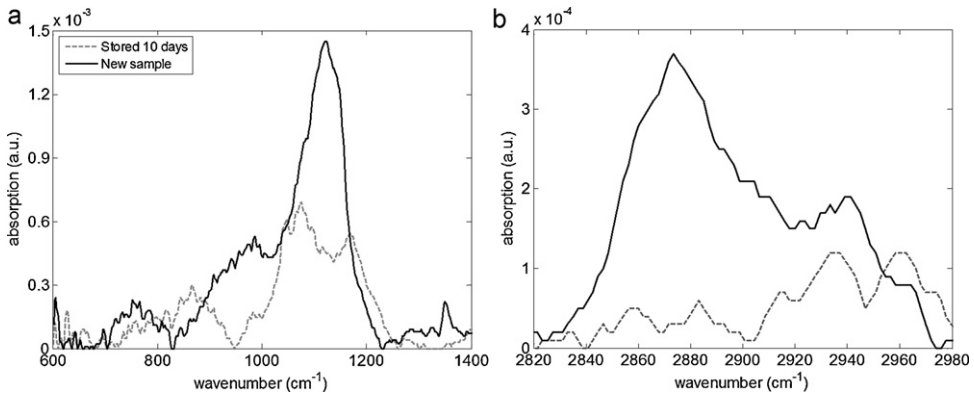

Fig. 4. IRRAS spectra for 1% biotinylated sensors showing the regions (a) 600–1400 cm^{-1} and (b) 2820–2980 cm^{-1}, comparing the spectrum obtained for a freshly prepared (solid line) sensor with a sensor stored for 10 days in light (dashed line).

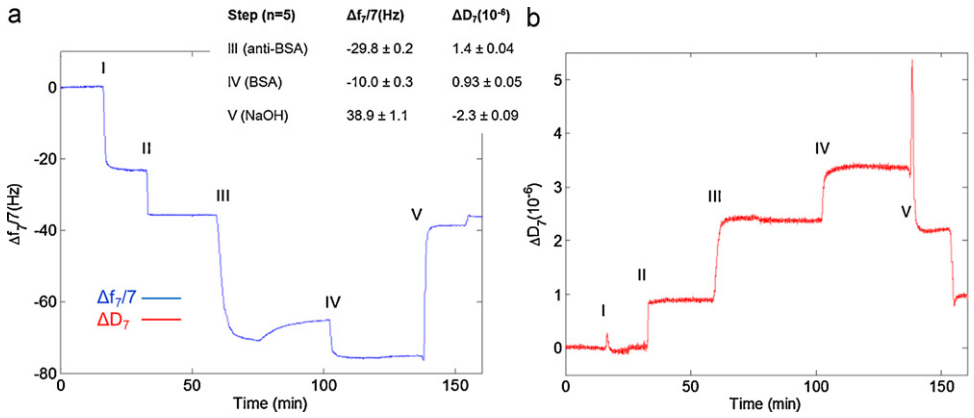

Fig. 5. QCM-D (a) frequency and (b) dissipation shifts for the immobilization of streptavidin (I), biotin-protein-A (II), anti-BSA (III) and BSA (IV) onto 1% biotinylated OEG monolayers. In step V anti-BSA and BSA were removed with NaOH. Averaged values and standard deviations are shown for steps III–V that were repeated 5 times in sequence to give a total measuring time of >600 min.

exposure to certain low molecular weight compounds were screened by QCM-D using the 1% biotinylated sensor (Nileback et al., 2010). There, small but specific shifts in dissipation could be detected as response to conformational changes by using inactivated plasminogen as reference and subtracting this background signal from the signal for the active protein. Together, these two applications examples provide good evidence that this kind of surface modification gives new possibilities for the QCM-D technology in the fields of biopharmaceutics.

4. Conclusions

Biotinylated sensors for QCM-D based sensing were prepared by forming mixed self-assembled monolayers of OEG disulfides on gold from a solution containing 1% of biotin end groups. This biotin fraction was concluded to be the most suitable for high performance measurements by very reproducibly binding a monolayer of streptavidin while being repellant to non-specific binding of serum proteins at high concentration. These sensors were stable for long-time measurements, regeneration protocols with 10 mM NaOH, as well as storage up to 8 weeks when stored in light-sealed bags at 2–8 °C. Exclusion of light access was concluded to be the most important parameter for storage stability. IRRAS studies showed that the molecular structure was composed of both helically and amorphous phases correlating well with the structure needed for resistance to unspecific protein adsorption. By IRRAS it was also possible to determine that the characteristic ethylene glycol structure had been lost for sensors stored for 10 days in light, further emphasizing that it is crucial to store this kind of sensors in the dark to ensure continued activity for a longer time. The biotinylated sensors proved to be stable for multiple antibody–antigen interactions in an automated QCM-D setup and together with an earlier study of plasminogen conformational changes using the same sensors this surface modification has proven to be a versatile and good template for protein interaction studies. In our view, QCM-D is an underexplored technique compared to other sensing techniques for detailed protein interaction studies. One key component for advancement of this field is controlled surface chemistry and the biotinylated sensors provided here fulfill many of the requirements for performing highly sensitive protein interaction analyses by QCM-D.

Acknowledgements

The authors would like to thank Tobias Ekblad at Linköping University for help with infrared spectroscopy measurements and prof. Bo Liedberg for providing his laboratory for IR measurements. R.V. acknowledges the support from the Swedish Institute (Visby program). This work was supported by the European Union Seventh Framework Programme (FP7/2007–2013) under grant agreement n° NMP4-SL-2009-229292 (Find&Bind).

References

Aung, K.M.M., Ho, X.N., Su, X.D., 2008. Sens. Actuator B: Chem. 131 (2), 371–378.
Azzaroni, O., Mir, M., Knoll, W., 2007. J. Phys. Chem. B 111 (48), 13499–13503.
Bingen, P., Wang, G., Steinmetz, N.F., Rodahl, M., Richter, R.P., 2008. Anal. Chem. 80 (23), 8880–8890.

Brewer, N.J., Janusz, S., Critchley, K., Evans, S.D., Leggett, G.J., 2005. J. Phys. Chem. B 109 (22), 11247–11256.
Collings, A.F., Caruso, F., 1997. Rep. Prog. Phys. 60 (11), 1397–1445.
Cooper, M.A., 2003. Anal. Bioanal. Chem. 377 (5), 834–842.
Dolatshahi-Pirouz, A., Rechendorff, K., Hovgaard, M.B., Foss, M., Chevallier, J., Besenbacher, F., 2008. Colloids Surf. B Biointerfaces 66 (1), 53–59.
Edvardsson, M., Svedhem, S., Wang, G., Richter, R., Rodahl, M., Kasemo, B., 2009. Anal. Chem. 81 (1), 349–361.
Feldman, K., Hahner, G., Spencer, N.D., Harder, P., Grunze, M., 1999. J. Am. Chem. Soc. 121 (43), 10134–10141.
Gobi, K.V., Matsumoto, K., Toko, K., Ikezaki, H., Miura, N., 2007. Anal. Bioanal. Chem. 387 (8), 2727–2735.
Harder, P., Grunze, M., Dahint, R., Whitesides, G.M., Laibinis, P.E., 1998. J. Phys. Chem. B 102 (2), 426–436.
Hendrickson, W.A., Pahler, A., Smith, J.L., Satow, Y., Merritt, E.A., Phizackerley, R.P., 1989. Proc. Natl. Acad. Sci. U. S. A. 86 (7), 2190–2194.
Hoa, X.D., Kirk, A.G., Tabrizian, M., 2007. Biosens. Bioelectron. 23 (2), 151–160.
Hook, F., Ray, A., Norden, B., Kasemo, B., 2001. Langmuir 17 (26), 8305–8312.
Huang, N.P., Voros, J., De Paul, S.M., Textor, M., Spencer, N.D., 2002. Langmuir 18 (1), 220–230.
Huang, R.P., Huang, R.C., Fan, Y., Lin, Y., 2001. Anal. Biochem. 294 (1), 55–62.
Johannsmann, D., Reviakine, I., Richter, R.P., 2009. Anal. Chem. 81 (19), 8167–8176.
Jonkheijm, P., Weinrich, D., Schroder, H., Niemeyer, C.M., Waldmann, H., 2008. Angew. Chem. Int. Ed. 47 (50), 9618–9647.
Laitinen, O.H., Hytonen, V.P., Nordlund, H.R., Kulomaa, M.S., 2006. Cell. Mol. Life Sci. 63 (24), 2992–3017.
Larsson, C., Rodahl, M., Hook, F., 2003. Anal. Chem. 75 (19), 5080–5087.
Lee, J.W., Sim, S.J., Cho, S.M., Lee, J., 2005. Biosens. Bioelectron. 20 (7), 1422–1427.
Luppa, P.B., Sokoll, L.J., Chan, D.W., 2001. Clin. Chim. Acta 314 (1–2), 1–26.
Nileback, E., Westberg, F., Deinum, J., Svedhem, S., 2010. Anal. Chem. 82 (20), 8374–8376.
Palegrosdemange, C., Simon, E.S., Prime, K.L., Whitesides, G.M., 1991. J. Am. Chem. Soc. 113 (1), 12–20.
Prieto-Simon, B., Campas, M., Marty, J.L., Noguer, T., 2008. Biosens. Bioelectron. 23 (7), 995–1002.
Prime, K.L., Whitesides, G.M., 1993. J. Am. Chem. Soc. 115 (23), 10714–10721.
Reviakine, I., Brisson, A., 2001. Langmuir 17 (26), 8293–8299.
Richter, R.P., Hock, K.K., Burkhartsmeyer, J., Boehm, H., Bingen, P., Wang, G.L., Steinmetz, N.F., Evans, D.J., Spatz, J.P., 2007. J. Am. Chem. Soc. 129 (17), 5306.
Rindzevicius, T., Alaverdyan, Y., Dahlin, A., Hook, F., Sutherland, D.S., Kall, M., 2005. Nano Lett. 5 (11), 2335–2339.
Seifert, M., Rinke, M.T., Galla, H.J., 2010. Langmuir 26 (9), 6386–6393.
Valiokas, R., Malysheva, L., Onipko, A., Lee, H.H., Ruzele, Z., Svedhem, S., Svensson, S.C.T., Gelius, U., Liedberg, B., 2009. J. Electron. Spectrosc. Relat. Phenom. 172 (1–3), 9–20.
Vanderah, D.J., Arsenault, J., La, H., Gates, R.S., Silin, V., Meuse, C.W., Valincius, G., 2003. Langmuir 19 (9), 3752–3756.
Vanderah, D.J., Walker, M.L., Rocco, M.A., Rubinson, K.A., 2008. Langmuir 24 (3), 826–829.
Welch, W., Ruppert, J., Jain, A.N., 1996. Chem. Biol. 3 (6), 449–462.
Vermette, P., Gengenbach, T., Divisekera, U., Kambouris, P.A., Griesser, H.J., Meagher, L., 2003. J. Colloid Interface Sci. 259 (1), 13–26.
Wilchek, M., Bayer, E.A., 1988. Anal. Biochem. 171 (1), 1–32.
Wilchek, M., Bayer, E.A., 1999. Biomol. Eng. 16 (1–4), 1–4.
Wolny, P.M., Banerji, S., Gounou, C., Brisson, A.R., Day, A.J., Jackson, D.G., Richter, R.P., 2010a. J. Biol. Chem. 285 (39), 30170–30180.
Wolny, P.M., Spatz, J.P., Richter, R.P., 2010b. Langmuir 26 (2), 1029–1034.
Vuignier, K., Schappler, J., Veuthey, J.L., Carrupt, P.A., Martel, S., 2010. Anal. Bioanal. Chem. 398 (1), 53–66.
Zhang, H.B., Shepherd, J.N.H., Nuzzo, R.G., 2010. Soft Matter 6 (10), 2238–2245.
Zhu, Z.R., Cuozzo, J., 2009. J. Biomol. Screen. 14 (10), 1157–1164.